



ELSEVIER

Available online at [www.sciencedirect.com](http://www.sciencedirect.com)

SCIENCE @ DIRECT®

International Journal of Psychophysiology 53 (2004) 105–119

INTERNATIONAL  
JOURNAL OF  
PSYCHOPHYSIOLOGY

[www.elsevier.com/locate/ijpsycho](http://www.elsevier.com/locate/ijpsycho)

# Automatic correction of ocular artifacts in the EEG: a comparison of regression-based and component-based methods<sup>☆</sup>

Garrick L. Wallstrom<sup>a,\*</sup>, Robert E. Kass<sup>b</sup>, Anita Miller<sup>c</sup>,  
Jeffrey F. Cohn<sup>d</sup>, Nathan A. Fox<sup>e</sup>

<sup>a</sup>Center for Biomedical Informatics, University of Pittsburgh, Forbes Tower Suite 8084, 200 Lothrop Street, Pittsburgh, PA 15213, USA

<sup>b</sup>Department of Statistics and the Center for the Neural Basis of Cognition, Carnegie Mellon University, Pittsburgh, PA, USA

<sup>c</sup>Department of Psychiatry and Psychology, University of Pittsburgh, Pittsburgh, PA, USA

<sup>d</sup>Department of Psychology, University of Pittsburgh, Pittsburgh, PA, USA

<sup>e</sup>Department of Human Development, University of Maryland, College Park, MD, USA

Received 27 February 2003; received in revised form 23 December 2003; accepted 11 March 2004

Available online 25 May 2004

## Abstract

A variety of procedures have been proposed to correct ocular artifacts in the electroencephalogram (EEG), including methods based on regression, principal components analysis (PCA) and independent component analysis (ICA). The current study compared these three methods, and it evaluated a modified regression approach using Bayesian adaptive regression splines to filter the electrooculogram (EOG) before computing correction factors. We applied each artifact correction procedure to real and simulated EEG data of varying epoch lengths and then quantified the impact of correction on spectral parameters of the EEG. We found that the adaptive filter improved regression-based artifact correction. An automated PCA method effectively reduced ocular artifacts and resulted in minimal spectral distortion, whereas ICA correction appeared to distort power between 5 and 20 Hz. In general, reducing the epoch length improved the accuracy of estimating spectral power in the alpha (7.5–12.5 Hz) and beta (12.5–19.5 Hz) bands, but it worsened the accuracy for power in the theta (3.5–7.5 Hz) band and distorted time domain features. Results supported the use of regression-based and PCA-based ocular artifact correction and suggested a need for further studies examining possible spectral distortion from ICA-based correction procedures.

© 2004 Elsevier B.V. All rights reserved.

**Keywords:** Electroencephalography; Ocular artifact; Regression; Principal components analysis; Independent components analysis; Adaptive filter

## 1. Introduction

Ocular activity creates significant artifacts in the electroencephalogram (EEG, Fisch, 1991). Epochs contaminated by ocular artifacts can be manually excised, but at the cost of intensive human labor and substantial data loss. Alternatively, correction procedures can distinguish brain electrical activity

<sup>☆</sup> Support for the current work was provided by NIMH Program Project MH56193, NSF VIGRE Award DMS-9819950, NIMH Postdoctoral Fellowship MH18951, NIMH Seed Award MH30915 and a NARSAD Young Investigator Award.

\* Corresponding author. Tel.: +1-412-647-7113; fax: +1-412-647-7190.

E-mail address: [garrick@cbmi.pitt.edu](mailto:garrick@cbmi.pitt.edu) (G.L. Wallstrom).

from ocular potentials, using regression-based or component-based models (see Croft and Barry, 2000; Lins et al., 1993a,b). However, the current literature lacks consensus about optimal correction procedures. This is due, in part, to the inherent challenges of developing and implementing accurate models. In addition, few studies have directly compared different methods for ocular artifact correction, and existing studies have focused almost exclusively on applications to event-related potential (ERP) research (Lins et al., 1993a,b). The goal of the current study was to use real and simulated EEG data to compare multiple regression, principal component and independent component methods of ocular artifact correction, with a particular emphasis on implications for spectral analyses of the EEG waveform.

Traditional ocular artifact correction procedures use a regression-based approach (Elbert et al., 1985; Gratton et al., 1983). Regression analyses are used to compute propagation factors or transmission coefficients in order to define the amplitude relation between one or more electrooculogram (EOG) channels and each EEG channel. Correction involves subtracting the estimated proportion of the EOG from the EEG. One concern often raised about the regression approach is bidirectional contamination. If ocular potentials can contaminate EEG recordings, then brain electrical activity can also contaminate the EOG recordings. Therefore, subtracting a linear combination of the recorded EOG from the EEG may not only remove ocular artifacts but also interesting cerebral activity. In order to reduce the cerebral activity in the EOG, Lins et al. (1993b) suggested low-pass filtering the EOG signal used to compute regression coefficients. However, they recognized that low-pass filtering removes all high frequency activity from the EOG signal, both of cerebral and ocular origin. In the current paper, we introduce a new filtering approach for regression-based correction using Bayesian adaptive regression splines (DiMatteo et al., 2001; Wallstrom et al., 2002). This approach uses a locally defined nonlinear filter to remove high frequency activity when the amplitude fluctuations are small and retain high frequency activity when the amplitude fluctuations are large. Such adaptively filtered EOG essentially isolates activity typically associated with ocular artifacts and removes cerebral activity. The use of

such adaptive filtering prior to applying regression correction may substantially reduce problems from bidirectional contamination.

Another class of methods is based on decomposing the EEG and EOG signals into spatial components, identifying artifactual components and reconstructing the EEG without the artifactual components. For example, Lins et al. (1993b) and Lagerlund et al. (1997) used principal component analysis (PCA) to identify the artifactual components. In addition, the dipole modeling technique of Berg and Scherg (1991a,b, 1994) can use PCA to compute topographies of eye activity. Statistically, PCA decomposes the signals into uncorrelated, but not necessarily independent, components that are spatially orthogonal. More importantly for the purpose of artifact correction, the PCA components may be thought of as formed sequentially to maximize the remaining variance. In particular, the first component is formed to have the largest variance, and therefore easily isolates large amplitude ocular artifacts. Such components can be identified and selected automatically by comparing them with the EOG signal, as we demonstrate in this paper. A newer approach uses independent component analysis (ICA), which was developed in the context of blind source separation problems to form components that are independent (Bell and Sejnowski, 1995; Comon, 1994; Jutten and Herault, 1991). ICA has been applied to correct for ocular artifacts, as well as artifacts generated by other sources (Jung et al., 1998a,b, 2000; Vigário, 1997). Compared to PCA, ICA removes the constraint of orthogonality and forces components to be approximately independent rather than simply uncorrelated. However, the ICA components lack the important variance maximization property possessed by PCA components. In addition, ICA requires the user to manually select components for correction, thus creating challenges for implementing automated correction routines.

In the current study, we compare the performance of regression-based and component-based correction procedures on real and simulated EEG data of varying epoch lengths. In particular, the correction procedures we consider are two time-domain regression methods (i.e., with and without adaptive filtering), automated and manual PCA, and ICA. Our

simulation study allows us to verify the effect of the adaptive filter on correction performance and observe the role of epoch length on the regression methods and automated PCA. In addition, we quantify the effects of each method on the spectral parameters of the EEG. Our aim is to describe the relative strengths and weaknesses of the different methods for effectively removing ocular artifact, without distorting the spectral parameters of the EEG by correction.

## 2. Materials and methods

### 2.1. Subjects

Twelve adult subjects were selected from subjects participating in a larger study of childhood-onset depression (Miller et al. (2002)). Half of the subjects had a history of childhood-onset depression and half had no history of major psychopathology. Within each diagnostic group, half of the subjects were female. The ages of the subjects range from 21 to 35, with a mean of 28. There were no significant age differences for the diagnostic and gender groups.

### 2.2. Recordings

EEG and EOG was recorded during three 60-s resting baseline periods with the eyes open. EEG data was acquired following standard guidelines (Pivik et al. (1993)). An electrode cap (ElectroCap, Eaton, OH) was positioned according to the expanded 10–20 International System. Electrodes were placed at sites F3, F4, AF3, AF4, F7, F8, FC1, FC2, FC5, FC6, C3, C4, T7, T8, P3, P4, P7, P8, O1 and O2. Recordings were made using the vertex (Cz) reference. The isolated-common ground was AFz. The EOG was recorded using a bipolar reference and six-mm tin electrodes. Electrodes were placed above and below the right eye to record the vertical EOG and on the outer canthi to record the horizontal EOG. Scalp electrode impedances were below 10 k $\Omega$  throughout the session. Data were collected with equipment and software from the James Long (Caroga Lake, NY). The bioamplifier was set for band-pass filtering with half power cutoff frequencies of 0.01 and 100 Hz (12 dB/octave

roll-off). The gain was 5000 for the EEG channels and 2500 for the EOG channels. Data were digitized at 512 Hz.

### 2.3. Simulation

In order to compare the correction procedures described above, we simulated forty 60-s realizations of EEG and EOG data. The simulation process for a 3-s realization is diagrammed in Fig. 1. For each realization, we began by simulating 10 independent potential sources, 8 cerebral, 1 horizontal ocular and 1 vertical ocular. We then created a random mixing matrix to enable the construction of the observed and true EEG and EOG channels.

To simulate a realization of a cerebral source, we began by selecting a random observed EEG channel for a randomly selected subject and randomly selected baseline period. We call this the pre-source EEG. We then simulated the EEG source by removing significant ocular artifacts from the pre-source via regression upon the unfiltered EOG using a 60-s epoch.

To simulate the ocular sources, we formed each pre-source EOG by selecting the corresponding EOG channel from a randomly selected subject and randomly selected baseline period. The EOG sources were then obtained by filtering the pre-source EOG using free knot splines. The 10 subjects, from which the EEG and EOG pre-sources were taken, were selected randomly, without replacement, from among the 12 subjects in the available set of data. Since each channel of source data was derived from a different subject, the 10 channels are truly independent.

Note that, aside from the artifact removal, we have used independent segments of observed EEG as cerebral sources. While there is no guarantee that the true cerebral sources resemble the potentials recorded on the scalp, this use of the observed EEG helps to ensure that the simulated scalp EEG resemble real EEG.

The observed EEG and EOG data are simulated by multiplying the simulated sources by a random weight matrix. The simulated observed channels are therefore linear combinations of the simulated cerebral and ocular sources. The EEG coefficient vectors are formed by normalizing vectors of independent

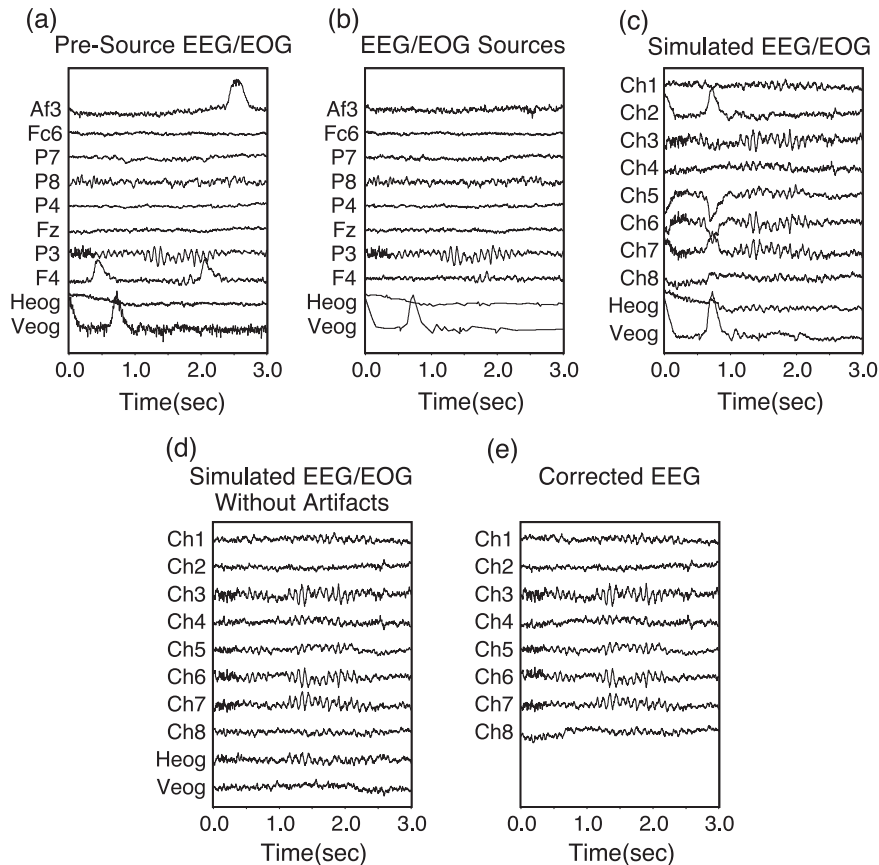


Fig. 1. The simulation process, shown for a 3-s epoch. (a) Each pre-source channel originates from a different, randomly selected subject. The EEG pre-sources were randomly selected 60-s realizations taken from randomly selected EEG channels. The EOG pre-sources were randomly selected 60-s realizations taken from the corresponding EOG channels. (b) Each EEG source was derived from the corresponding EEG pre-source by applying an artifact correction procedure (REG-RAW). Each EOG source was derived from the corresponding EOG pre-source by applying the adaptive filter. (c) The simulated EEG/EOG was obtained by multiplying the EEG/EOG sources by a random weight matrix. (d) To simulate the EEG and EOG that would have been observed in the absence of artifacts, the EEG/EOG sources were multiplied by the same weight matrix, modified by replacing the EEG source coefficients with zeroes. (e) The corrected EEG was obtained by applying an artifact correction procedure to the simulated EEG/EOG. This corrected EEG was then compared to the EEG/EOG simulated without artifacts given in (d).

standard normal random variates. The EOG coefficient vectors require additional care. Since each EOG is primarily a measure of ocular potentials, it is important that each of the two ocular sources contributes substantially to its respective observed EOG channel. This suggests heavily weighting the contribution from the corresponding ocular source. On the other hand, the observed EOG should contain a similar amount of noise as the observed EEG, suggesting that there should still be considerable non-ocular contributions. We therefore set the coefficient of the corresponding ocular source to be 1.

The remaining coefficients are formed from independent standard normal random variates, scaled so that the squared norm of the remaining coefficients is 0.9. Therefore, for both EOG and EEG, the expected squared coefficient of a cerebral source is 0.1.

To evaluate the performance of the correction procedures, we need to create the true EEG that corresponds to the simulated observed EEG. This can be accomplished by multiplying the simulated sources by the weight matrix formed above with the cerebral source coefficients replaced with zeroes.

#### 2.4. Artifact correction

In this section, we describe five methods for ocular artifact correction. Two are based upon regression analysis (REG-RAW and REGADAPT), two upon principal components analysis (PCA-MAN and PCA-AUTO) and one upon independent components analysis (ICA-MAN). All of the correction procedures are applied to epochs whose lengths may be less than that of the whole realization. Within an epoch, each channel of EEG and EOG is centered to have zero-mean before the correction procedures are applied. Given the available data, the EOG consists here of two bipolar referenced channels. Additional or alternative EOG channels could be easily used with these methods.

Two of the above methods require manual guidance, PCA-MAN and ICA-MAN. We only apply these two methods to the entire realization. The others, REG-RAW, REG-ADAPT and PCA-AUTO, are automatic, which permits multiple application to small epochs. For these, we used three epoch lengths: 60, 10 and 1 s. When the epoch length is smaller than the realization, we use epochs that overlap by 50%. The overlap of epochs allows the corrected epochs to be combined into a single continuous corrected realization (see Appendix A).

#### 2.5. Regression-based approaches to correction

Two correction procedures based on regression in the time domain were studied. Each procedure uses the following linear model to approximate the relationship between the observed EOG, the observed EEG and the true unobserved EEG, where by ‘true’ EEG, we mean the signal that would have been recorded in the absence of ocular artifacts.

$$\text{OBS}_i(t) = \alpha_{1i}F(\text{HEOG})(t) + \alpha_{2i}F(\text{VEOG})(t) + \text{EEG}_i(t),$$

where  $\text{OBS}_i(t)$  denotes the observed EEG recording from lead  $i$  at time  $t$ ,  $\text{HEOG}(t)$  and  $\text{VEOG}(t)$  denote the observed recordings at time  $t$  from the horizontal and vertical EOG channels, respectively, and  $\text{EEG}_i(t)$  denotes the true unobserved EEG from lead  $i$  at time  $t$ . In the above equation,  $F(\cdot)$  denotes a procedure-dependent filter.

Multiple regression may be used to estimate  $\alpha_{1i}$  and  $\alpha_{2i}$ . The estimated true EEG is then formed according to

$$\begin{aligned} \text{E}\hat{\text{E}}G_i(t) = & \text{OBS}_i(t) - \hat{\alpha}_{1i}F(\text{HEOG})(t) \\ & - \hat{\alpha}_{2i}F(\text{VEOG})(t). \end{aligned}$$

The correction procedure, REG-RAW, uses the unfiltered EOG channels in the regression. The procedure, REG-ADAPT, adaptively filters the EOG prior to correcting via regression. The adaptive filter that we employ uses a free-knot cubic spline to smooth each EOG realization. Cubic splines are continuous piecewise cubic functions. The points at which the functions meet are called knots. [deBoor \(1978\)](#) provides a detailed treatment of splines. Fixed-knot splines have the number of knots and their locations fixed in advance. With free-knot splines, the number of knots and their locations are estimated from the data. To fit the splines, we use the Bayesian formulation of [DiMatteo et al. \(2001\)](#). The advantage to using free-knot splines rather than fixed-knot splines is that the knots are placed adaptively where needed in order to provide a good smooth of the data. Specifically, knots should tend to be placed around large amplitude artifacts and few knots should be required in artifact-free regions. This adaptive feature of free-knot splines permits filtering the EOG of high frequency, small amplitude cerebral signals while retaining high frequency, large amplitude artifacts. Additional details can be found in [Wallstrom et al. \(2002\)](#).

[Fig. 2](#) contains an example of an adaptively filtered vertical EOG channel using this method. It can be seen that the essential features of the artifact are transferred to the filtered EOG unadulterated while the high frequency activity is filtered out.

#### 2.6. Component-based approaches to correction

The notion that potential differences measured on the scalp are attributable to a number of cerebral and artifactual (non-cerebral) electrical sources is conceptually appealing. Component-based approaches to artifact correction in EEG are based on estimating the contributions from these sources to the observed EEG. By identifying the estimated sources that cor-

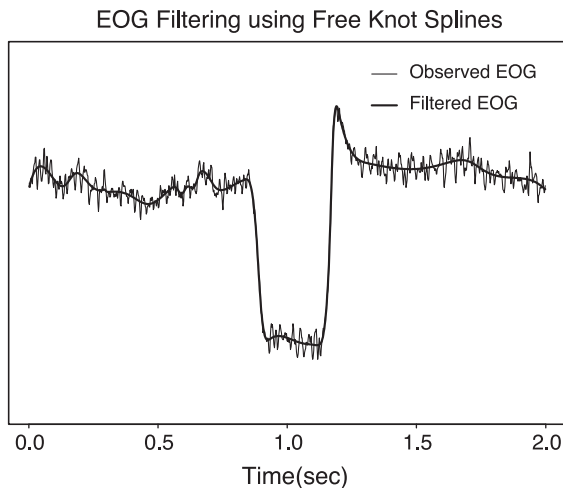


Fig. 2. Adaptive filtering of a 2-s epoch of vertical EOG using free-knot splines. The raw unfiltered EOG and the adaptively filtered EOG are displayed.

respond to artifacts, the effects of the artifacts can be removed. In general, source components (or simply, components) are linear combinations of the EEG and EOG channels, formed to have particular properties. Vectors of the coefficients give the spatial directions of the components. While the relative contributions of the channels to a component are meaningful, the overall strength (i.e. scale) of a component cannot be uniquely determined. The coefficient vectors are typically normalized to have length 1 in order to remove this indeterminacy. We may therefore think of the coefficient vectors as defining a new set of coordinate axes, and the components are simply the projections of the data onto these axes.

To formalize, let  $p$  be the total number of EEG and EOG channels used and  $n$  be the number of sample time points in the epoch. The data can then be represented by an  $n \times p$  matrix  $X$ . We form a  $p \times p$  matrix  $W$  whose columns are the coefficient vectors for the components. The components are then the columns of the  $n \times p$  matrix  $C = XW$ . After the formation of the components, those associated with artifacts must then be identified. Previously, identification had been performed manually by plotting the components and selecting those that resemble artifacts. An automated method for identification of ocular artifactual components is described below. After the artifactual components have been identified, the effect of these

components may be removed easily as follows. Let  $\tilde{X} = \tilde{C}W^{-1}$  where  $\tilde{C}$  is formed by replacing the artifactual components with zero vectors. The columns of  $\tilde{X}$  contain the corrected EEG and EOG data.

PCA and ICA are two approaches to constructing the matrix  $W$ . In PCA, each coefficient vector is formed so that the corresponding component has the largest sample variance, subject to the constraint that the component is uncorrelated with each of the preceding components. In particular, the first column of  $W$  contains the coefficients for the linear combination of the channels with maximum sample variance. The coefficient vectors constructed in this manner are simply the normalized eigenvectors of the sample covariance matrix, and as such, are necessarily orthogonal. In ICA, the coefficient vectors are formed so that the corresponding components are approximately statistically independent. A variety of iterative algorithms for ICA exist, including those by Bell and Sejnowski (1995), Hyvärinen and Oja (1997) and Lee et al. (1999). We used the fastICA algorithm of Hyvärinen (1999), implemented in the fastICA package by Marchini et al. (2002).

The components formed by ICA and PCA differ in three significant ways. First, the ICA components are independent, not just uncorrelated. Hence, while the PCA coefficient vectors depend only on second order moments, the ICA coefficient vectors are necessarily driven by higher order moments. The assumption that the distinct cerebral and artifactual source components are independent is appealing, making ICA an attractive approach. Second, the ICA coefficient vectors are not necessarily orthogonal. A consequence of PCA is that the constructed components lie on orthogonal axes. However, the underlying electrical sources need not be spatially orthogonal. Third, the PCA components are specifically constructed to isolate sources of large variance. There is no reason to believe that the underlying electric sources share this variance maximization property. For example, the underlying sources may contribute equally to the total variance. These considerations make ICA appear to be more consistent with the assumptions of electric source components and, as a result, ICA has received widespread interest for use in artifact correction. However, the variance maximization property of PCA seems particularly desirable for the isolation

of common ocular artifacts, which generally appear as large amplitude fluctuations. One purpose of the current study is to compare the relative effectiveness of ICA and PCA for ocular artifact correction.

The component-based procedures require the identification of artifactual components. Manual selection of components is used in the procedures PCA-MAN and ICA-MAN. In PCA-AUTO, the selection process is automated as follows. Since we are concerned here only with ocular artifacts and the EOG is a reliable indicator of ocular movements, we select components that are highly correlated with the observed EOG. Specifically, each component is regressed upon the two observed EOG channels and we identify components as artifactual when the squared multiple correlation coefficient ( $R^2$ ) exceeds a cutoff value. We experimented with the value of the cutoff and found that  $R^2=0.95$  was effective in identifying artifactual components when using PCA.

This automatic selection method was not useful for selecting components formed from ICA. The effectiveness of the selection method relies on there being only a few artifactual components of ocular origin. This is because as the number of artifactual components increases, the components tend to be less correlated with the observed EOG channels, and therefore more difficult to identify as artifactual. Lowering the  $R^2$  cutoff would help, but it would also increase the chance for removal of cerebral sources. The components formed from PCA rarely contain more than two artifactual components. On the other hand, ICA often separates ocular activity into multiple sources.

### 2.7. Data quantification

To evaluate the artifact correction procedures we investigated errors in both the time and frequency domains. In the time domain we calculated, for each channel, the mean squared error between the true EEG and the corrected EEG. When overlapping epochs were used, the corrected epochs were first aligned to create a single continuous corrected realization.

In the frequency domain, for each channel we estimate power density (in dB) for three frequency bands, theta (3.5–7.5 Hz), alpha (7.5–12.5 Hz) and beta (12.5–19.5 Hz). Specifically, the EEG was average referenced and power was estimated using a

Hanning window taper on 1-s epochs with 50% overlap. For each epoch and frequency band, power density was formed by averaging the power estimates for frequencies within the band. Average power density was then computed by averaging the power density over all overlapping epochs and converting to decibels. For each correction method, we computed power density errors for each channel and frequency band.

Log-transformed correction errors were analyzed using a mixed model that accounted for dependencies imposed by the experimental design for the simulation. A separate analysis was performed for each measure of error. Reported significance levels were computed upon Tukey's HSD procedure, which accounts for multiple comparisons.

## 3. Results

### 3.1. Simulation results

The time and frequency domain errors are summarized in Table 1. The main findings are: adaptive EOG filtering reduces alpha and beta band errors, short epochs reduce frequency domain errors but enlarge time domain errors, and the component-based methods generally yield smaller theta band errors. Overall,

Table 1  
Table of mean correction errors by method

	Theta band	Alpha band	Beta band	Time domain ( $\mu$ V)
NO-CORR	4.93	0.65	0.25	25.20
REG-RAW-60	2.76	1.56	1.24	9.64
REG-RAW-01	2.39	1.43	1.03	20.14
REG-ADAPT-60	2.82	0.57	0.30	8.98
REG-ADAPT-01	2.30	0.44	0.25	16.06
PCA-MAN-60	1.58	1.72	1.60	9.85
PCA-AUTO-60	1.40	0.89	0.81	10.25
PCA-AUTO-10	1.21	0.65	0.64	11.43
PCA-AUTO-01	0.91	0.38	0.36	23.52
ICA-MAN-60	1.94	1.57	1.56	11.62

Each column displays the mean error for each of the nine correction methods and for no correction. The first three columns use frequency domain measures of error, specifically the mean absolute error in terms of power within the theta (3.5–7.5 Hz), alpha (7.5–12.5 Hz) and beta (12.5–19.5 Hz) bands. The fourth column uses a time domain measure of error, specifically the mean square root of the mean squared error.

the methods and epoch lengths with low error rates are REG-ADAPT with short and long epochs, and PCA-AUTO with short epochs, depending upon the EEG feature of interest.

There is little artifact in the beta band, 12.5–19.5 Hz, as indicated by the low mean absolute error when no correction is performed. Not correcting has the lowest mean absolute error among all of the methods (each  $p < 0.001$ ). Not correcting excluded, REG-ADAPT using 1- and 60-s epochs, and PCA-AUTO using 1-s epochs perform the best. Each of these three methods has lower mean error than each of the remaining methods (each  $p < 0.001$ ), and there is no difference among these three methods (each  $p > 0.750$ ).

In the alpha band, 7.5–12.5 Hz, not correcting and PCA-AUTO using 1-s epochs perform the best, with no difference between the two methods ( $p > 0.999$ ). These

two methods each has lower mean error than the remaining methods (for comparison to REG-ADAPT using 1-s epochs,  $p = 0.005$  and  $p = 0.032$ , respectively; for all other methods, each  $p < 0.001$ ). Excluding not correcting and PCA-AUTO using 1-s epochs, REG-ADAPT using 1-s epochs has the lowest mean error among the remaining methods (each  $p < 0.001$ ).

In the theta band, 3.5–7.5 Hz, PCA-AUTO using 1-s epochs has a lower mean error than all of the other methods (each  $p < 0.001$ , except  $p = 0.015$  for the comparison to PCA-AUTO using 10-s epochs). Every PCA and ICA method has a lower mean error than each of the regression methods (each  $p < 0.001$ ). Every correction method has a lower mean error than not correcting the EEG (each  $p < 0.001$ ).

In the time domain, we observe that the largest influence on the time domain error rates is the epoch

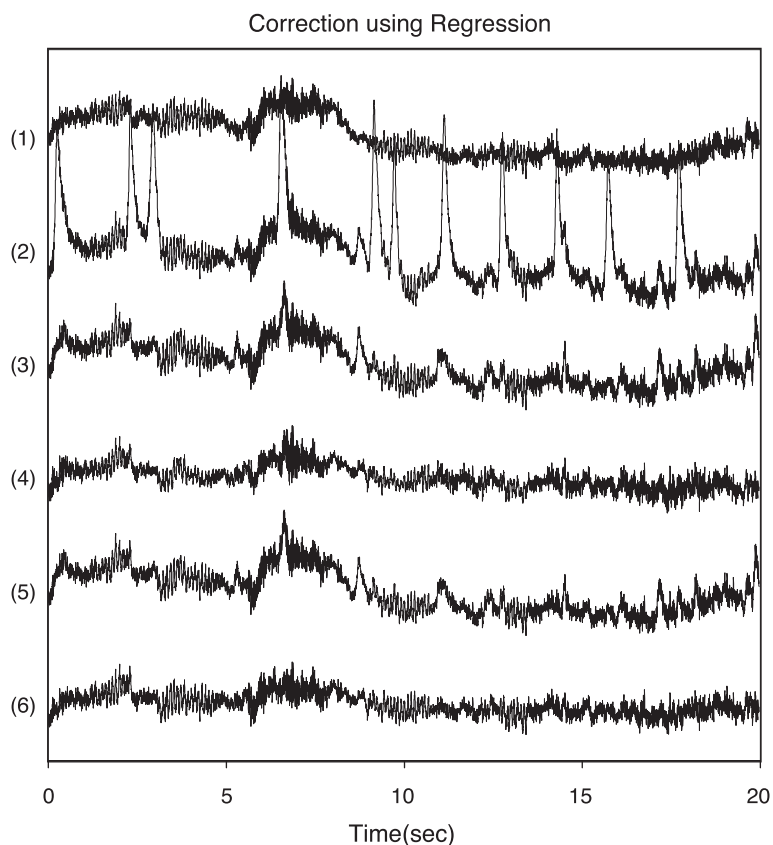


Fig. 3. Shown are the true signal (1), the observed signal (2) and four corrections: REG-RAW using a 60-s epoch (3), REG-RAW using a 1-s epoch (4), REG-ADAPT using a 60-s epoch (5) and REG-ADAPT using a 1-s epoch (6).

length. REG-RAW, REG-ADAPT and PCA-AUTO using 60-s epochs have lower mean error than their respective counterparts using 1-s epochs (each  $p < 0.001$ ). Furthermore, all methods that used 60-s epochs have lower mean error than not correcting the EEG (each  $p < 0.001$ ).

We now consider two examples from the simulation study. The first example, shown in Figs. 3 and 4, contrasts REG-RAW and REG-ADAPT using both 60- and 1-s epochs. The figures are based upon looking at only the first 20 s of the 60-s epoch. In Fig. 3, we see that all four methods do a fair to good job of removing the artifacts. While the 1-s epoch versions remove the individual blinks more completely than the 60-s epoch versions, the 1-s versions fail to reconstruct the low frequency temporal structure of the true EEG. This can be most readily observed by looking at the period from 18 to 20 s, and also at the period of high frequency activity between 6 and 8 s. The differences between

REG-RAW and REG-ADAPT are very difficult to observe in Fig. 3. However, if we consider the errors in the frequency domain, the differences are more apparent. Fig. 4 displays the error in log power, expressed in decibels, for the four correction methods. Here, it can be seen that above say, 10 Hz, use of the adaptive filter improves correction. The actual log power estimates for all of the correction methods, the true EEG, and no correction are displayed in Table 2.

The second example from the simulation study is displayed in Fig. 5, with log power estimates provided in Table 3. Displayed in Fig. 5, along with the true and observed signal, are the corrections made using REG-ADAPT with 1-s epochs, PCA-AUTO with 60-, 10- and 1-s epochs, and ICA-MAN. It can be seen that REG-ADAPT performs very well in the mid and high (alpha and beta) frequency bands, but is unable to reconstruct the low frequency character of the signal. PCA-AUTO with 60- and 10-s epochs perform poorly

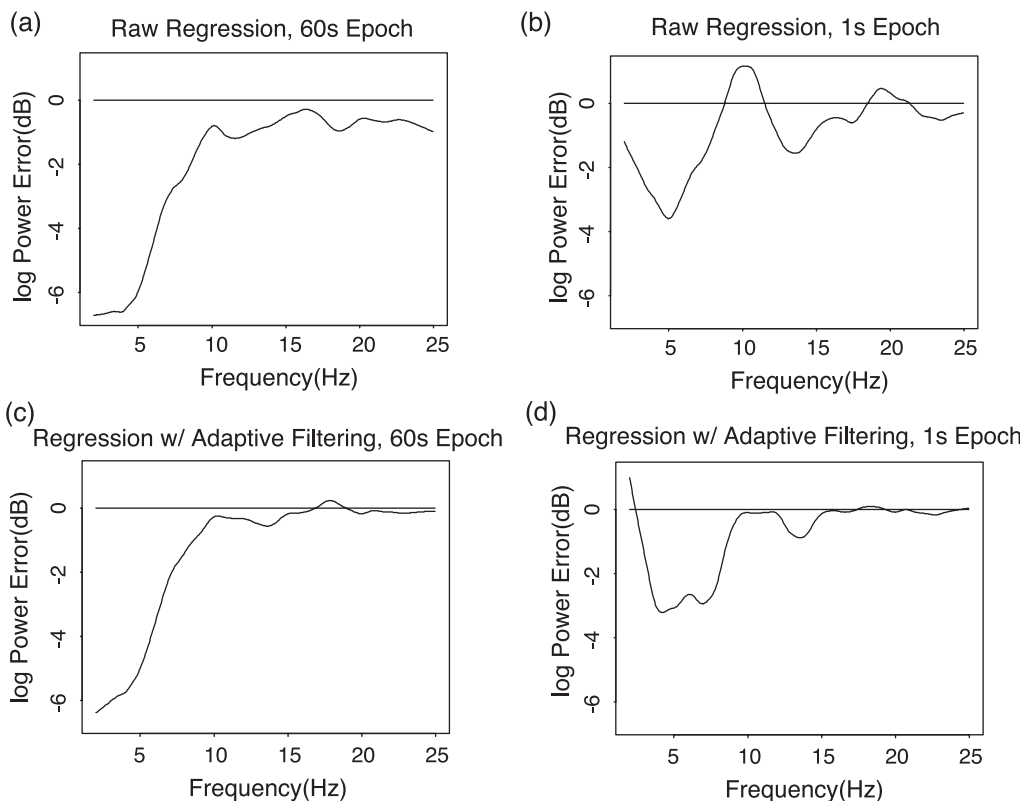


Fig. 4. The error in log power, expressed in decibels, is plotted against frequency for REG-RAW using a 60-s epoch (a), REG-RAW using 1-s epochs (b), REG-ADAPT using a 60-s epoch (c) and REG-ADAPT using 1-s epochs (d).

Table 2  
Table of log power estimates and time domain error by method for the first simulation example

	Theta band (dB)	Alpha band (dB)	Beta band (dB)	Time domain error ( $\mu$ V)
TRUTH	– 124.25	– 118.87	– 127.67	–
NO-CORR	– 113.12	– 118.35	– 127.61	65.36
REG-RAW-60	– 121.57	– 118.24	– 127.32	19.42
REG-RAW-01	– 121.94	– 119.93	– 126.99	18.92
REG-ADAPT-60	– 121.97	– 118.72	– 127.59	17.84
REG-ADAPT-01	– 122.29	– 118.56	– 127.46	16.94
PCA-MAN-60	– 122.73	– 118.44	– 127.47	9.32
PCA-AUTO-60	– 122.08	– 118.86	– 127.62	19.00
PCA-AUTO-10	– 122.16	– 118.85	– 127.61	18.84
PCA-AUTO-01	– 122.58	– 118.82	– 127.61	15.50
ICA-MAN-60	– 123.27	– 120.76	– 127.77	15.87

Values are given for the true unobservable signal, the observed signal (i.e., no correction used), and each of the nine correction methods. The first three columns give the estimated log power within the theta (3.5–7.5 Hz), alpha (7.5–12.5 Hz) and beta (12.5–19.5 Hz) bands. The fourth column gives the square root of the mean squared error. In this example, there is very little artifact in the alpha and beta bands. With the possible exception of REG-RAW on 1-s epochs, all of the methods provide a good estimate of beta power. With the exception of ICA-MAN, all of the methods estimate alpha power well. None of the methods do well at estimating theta band power, but ICA-MAN performed better than the others.

in the alpha and beta bands, but with 1-s epochs performs quite well. On the other hand, with 1-s epochs, the temporal structure is greatly distorted. Finally, ICA-MAN can be seen to result in a corrected signal with exaggerated theta, alpha and beta band activity.

### 3.2. Results with real data

An example with real data is displayed in Figs. 6 and 7. The data are 60 s of 21-channel EEG collected during a resting, eyes-open baseline condition. Two EOG channels were simultaneously recorded. Correction was performed using the entire 60 s of 23-channel data; however, only the first 10 s of 6 EEG and 2 EOG channels are displayed. The major ocular artifacts in the sample are a blink artifact in the first second, and eye movement artifacts between the sixth and eighth second marks.

The example demonstrates the performance of REG-ADAPT and PCA-AUTO with 1-s epochs, and

ICA-MAN using a 60-s epoch on real data. All three methods have removed the large amplitude changes associated with the artifacts (Fig. 6). However, the frequency domain characteristics of the ICA-corrected EEG are inconsistent with the observed EEG. The excessive high frequency power in the corrected F8 and AF4 channels can be observed in Fig. 6. Even the F7 channel, which appears in Fig. 6 to not be similarly affected, contains excessive power between 5 and 20 Hz (Fig. 7).

## 4. Discussion

### 4.1. Careful adaptive filtering improves correction when using regression in the time domain

We have argued that the use of an appropriate adaptive filter can improve correction when using a time domain regression approach to EEG correction. Adaptive filtering reduced the alpha band error rates by 63% and 69% when using 60- and 1-s epochs, respectively, and reduced the beta band error rates by 76% for both epoch lengths. It is important to emphasize, however, that adaptive filtering cannot completely remove the concern about bidirectional contamination. Low frequency contamination remains a problem for the regression approach. Adaptive filtering does substantially remove our concern about high frequency contamination of the EEG by ocular sources.

### 4.2. Automatic component selection with PCA is effective

With PCA, the automatic method of component selection was quite successful. We used a squared multiple correlation cutoff of  $R^2=0.95$ . The cutoff value may need to be adjusted depending on the epoch length, the number of EEG and EOG channels, and the nature of the EEG data. For the higher frequencies, little correction is generally needed so a conservative rule for the removal of components is not dangerous. When an artifact has considerable low frequency power, PCA rarely has a difficult time separating out the component and will therefore produce a large value of  $R^2$  for that component. Hence, it is probably better to err on the side of a large cutoff resulting in the conservative removal of components.

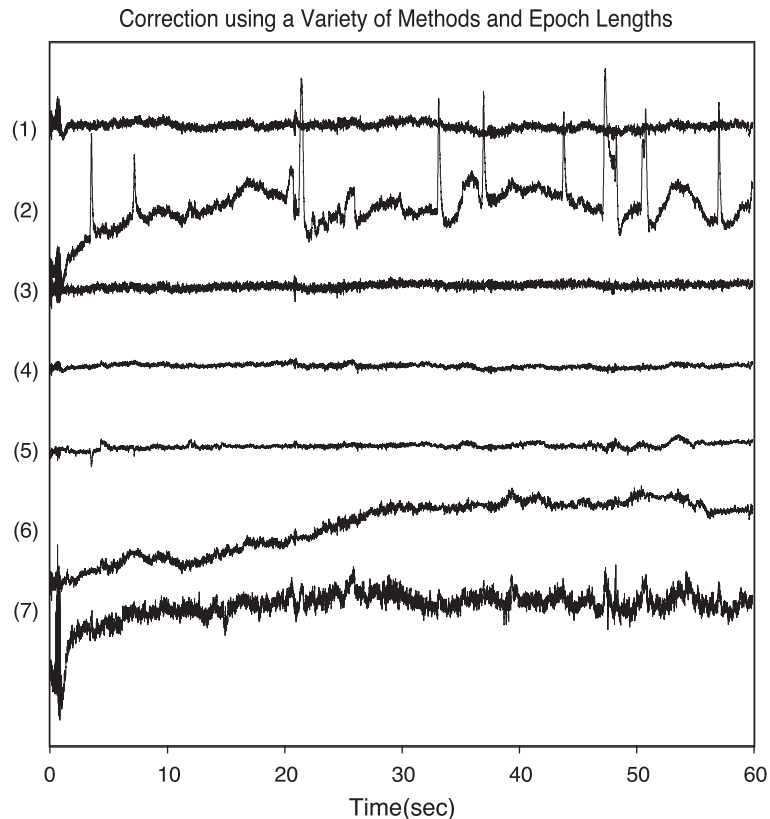


Fig. 5. Shown are the true signal (1), the observed signal (2) and five corrections: REG-ADAPT using 1-s epochs (3), PCA-AUTO using a 60-s epoch (4), PCA-AUTO using 10-s epochs (5), PCA-AUTO using 1-s epochs (6) and ICA-MAN using a 60-s epoch (7).

Automatic selection with 60-s epochs was more effective than manual selection with 60-s epochs. Manual selection, as we performed it, was based on visual comparisons between the EOG and the components. The components deemed artifactual were those that resembled the EOG in the time domain. Frequency domain characteristics that would affect the value of  $R^2$  may be difficult to see in the time domain and easier to dismiss than time domain characteristics. This suggests that the visual identification of components should use both time and frequency-domain displays.

#### 4.3. Epoch length should be selected based upon the quantities of interest

For both the regression-based and the component-based correction procedures, it is assumed that

certain relationships among the EEG and EOG channels and their cerebral and ocular sources are both linear and stationary over the epoch. For the regression approach without adaptive filtering, the model implies that the relationships between each EEG channel and the EOG channels are linear and remain constant over the entire epoch. When adaptive filtering is used with regression, the statistical model implies that the relationships between each EEG channel and the ocular sources are linear and remain constant throughout the epoch. The models for the component-based procedures imply that the relationships between each EEG and EOG channel and the cerebral and ocular sources are linear and constant over the epoch.

Our simulation study results showed that the use of short epochs improved estimation of power for the theta, alpha and beta bands, while wors-

Table 3  
Table of log power estimates and time domain error by method for the second simulation example

	Theta band (dB)	Alpha band (dB)	Beta band (dB)	Time domain error ( $\mu$ V)
TRUTH	–129.31	–129.48	–134.92	–
NO-CORR	–117.71	–127.59	–133.91	66.84
REG-RAW-60	–125.82	–131.40	–135.54	8.37
REG-RAW-01	–126.59	–131.58	–135.67	14.08
REG-ADAPT-60	–125.55	–129.32	–134.42	7.58
REG-ADAPT-01	–126.10	–129.43	–134.39	10.08
PCA-MAN-60	–134.61	–135.37	–139.33	7.19
PCA-AUTO-60	–134.61	–135.37	–139.33	7.19
PCA-AUTO-10	–131.05	–135.01	–139.33	11.45
PCA-AUTO-01	–126.63	–129.50	–135.33	73.04
ICA-MAN-60	–122.55	–121.86	–127.61	42.55

Values are given for the true unobservable signal, the observed signal (i.e., no correction used), and each of the nine correction methods. The first three columns give the estimated log power within the theta (3.5–7.5 Hz), alpha (7.5–12.5 Hz) and beta (12.5–19.5 Hz) bands. The fourth column gives the square root of the mean squared error. In this example, there is a non-negligible amount of alpha and beta band artifact. In the alpha and beta bands, REG-ADAPT provides the best estimates of power, followed by PCA-AUTO on 1-s epochs and REG-RAW. PCA-MAN, PCA-AUTO on 60- and 10-s epochs, and ICA-MAN give poor estimates of alpha and beta power. For the theta band, none of the methods give good estimates.

ening estimation of time domain characteristics due to the problem of re-attaching the corrected epochs. The improvement throughout the frequency bands of general interest strongly suggests that the relationships are not both linear and stationary. In effect, the use of a short epoch assumes that the relationships are piecewise-linear and piecewise-stationary throughout the realization. In much the same way that a step function can approximate a curve, the piecewise models may better approximate the true relationships among the channels and sources.

Our simulation study found improvements from the use of short epochs for both the regression-based approaches and for the automatic PCA technique. The magnitudes of the improvements were smaller for regression than for PCA. For regression, use of a 1-s epoch rather than a 60-s epoch reduced the mean absolute error for the theta, alpha and beta bands by between 8% and 23%, depending on the band and filtering. For automatic PCA, use of a 1-s

epoch reduced the mean absolute error by between 35% and 57%, depending on the band. This suggests that the assumptions of linearity and stationarity over 1 min is less problematic for the regression approaches than for component-based procedures.

In some studies, however, it may be important to assume that the relationships are stationary. If the primary interest is in EEG that occurs simultaneously with ocular activity, such as a startle response, the assumption of stationarity is critical to the correction of the EEG that coincides with the ocular activity. For other experimental conditions, such as a resting baseline or a non-visual oriented task, short epochs should be used for correction before calculating quantities based on frequencies over 3.5 Hz, such as alpha band asymmetries.

#### 4.4. Spectral distortions and ICA

We were disappointed by the performance of ICA for artifact correction, both in our simulation study and in investigations with real data. In addition to the fastICA algorithm of Hyvärinen (1999), we also experimented with the extended ICA algorithm of Jung et al. (1998a) and implemented by Makeig et al. (1998). The problem of spectral power overestimation, as shown in Figs. 6 and 7, was more common with extended ICA than with fastICA.

It may be that other ICA algorithm variants may produce more successful artifact correction. At this point we, are only left to conclude that the assumption of independence of the ocular and cerebral sources is not strong enough to isolate the ocular sources well. The use of epochs substantially longer than the 60-s epochs that we used may hold the key to the success of ICA for artifact correction.

It worth emphasizing that this study only considered one application of ICA, and our conclusions should not be taken as a general statement about the performance of ICA. Future studies are needed to further investigate the potential spectral distortions induced by ICA.

#### 4.5. Limitations and future directions

This study used two bipolar referenced EOG channels. However, Elbert et al. (1985) suggest that

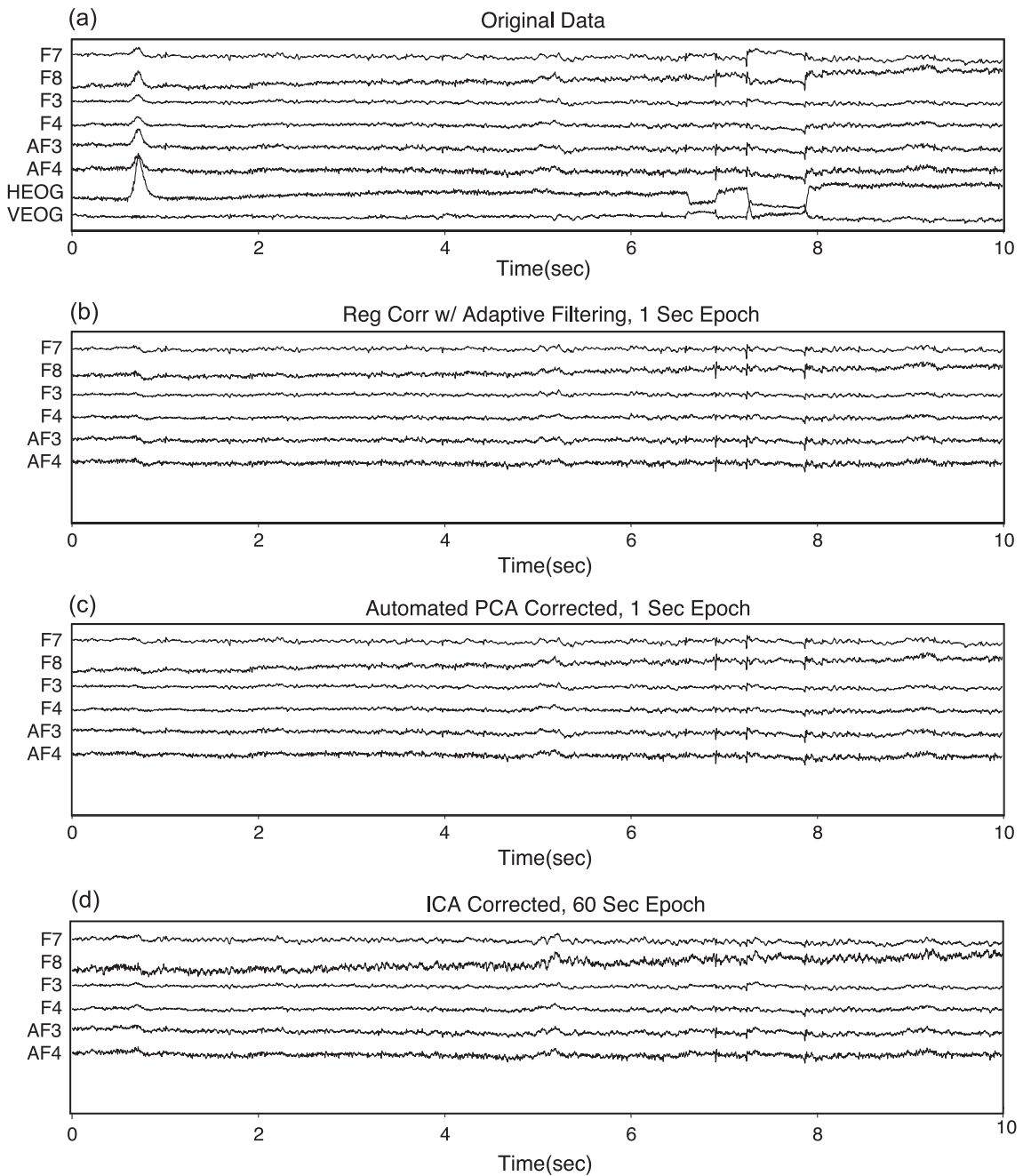


Fig. 6. The original data contained 60 s of 21 EEG and 2 EOG channels collected during a resting baseline condition. (a) Selected channels for the first 10 s of the original data. (b) The corrected channels using REG-ADAPT-01 (b), AUTO-PCA-01 (c) and ICA-60 (d).

at least three EOG channels are needed to correctly differentiate artifact types. Future studies should include a radial EOG channel to distinguish blinks

and vertical saccades. Furthermore, increasing the number of simulated ocular sources may improve the EEG simulations.

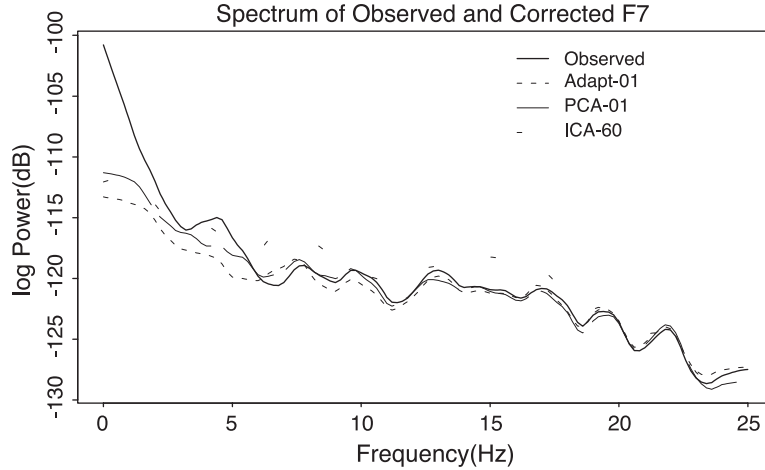


Fig. 7. The spectra of observed and corrected F7 channel using REG-ADAPT-01, AUTO-PCA-01 and ICA-60.

Although we only examined adult data here, the simulation results for the theta band suggest that artifact correction may be more delicate for child EEG, where peak alpha activity occurs around 7 Hz. Future work should examine the implications of artifact correction for spectral analyses of child EEG data.

### Appendix A. Reconciling overlapping signals

A consequence of using a method that operates on small overlapping portions of an epoch is a need to reconcile the corrected portions at the end. This appendix describes the procedure we used. To simplify the discussion, for now suppose that there are two signals defined on overlapping epochs where each signal was formed by applying a correction method to the observed EEG channel. Let  $S_1(t)$  denote the first signal, defined for  $t_0 < t \leq t_2$ , and  $S_2(t)$  denote the second signal, defined for  $t_1 < t \leq t_3$ . We are interested in reconciling  $S_1(t)$  and  $S_2(t)$  for  $t_1 < t \leq t_2$ . As each of the correction methods discussed herein amount to subtracting a linear combination of the EEG and possibly filtered EOG channels, the difference between  $S_1$  and  $S_2$  in the overlap region is also a linear combination of the EEG and possibly filtered EOG channels. While the EEG and EOG are centered prior to correction on

each epoch, the channels need not have zero mean on the overlap portion of the epoch. It follows that in the overlap region,  $S_1$  and  $S_2$  are not mutually centered. Therefore the reconciliation procedure that we use contains two steps.

- (i) Vertically shift  $S_2$  so that  $S_1$  and  $S_2$  have the same center in the overlap region.
- (ii) Form a single signal  $S$  such that in the overlap region  $S$  is a weighted average of  $S_1$  and  $S_2$ .

For step (i), we simply define  $S_2^*(t) = S_2(t) - m_2 + m_1$ , where  $m_1$  and  $m_2$  are the respective means of  $S_1$  and  $S_2$  in the overlap region. For step (ii), let  $w(x)$  be a continuous weight function defined for  $0 \leq x \leq 1$  such that  $w(0) = 0$  and  $w(1) = 1$ , and define

$$S(t) = \begin{cases} S_1(t), & t_0 < t \leq t_1 \\ S_1(t) \left[ 1 - w\left(\frac{t-t_1}{t_2-t_1}\right) \right] + S_2^*(t) w\left(\frac{t-t_1}{t_2-t_1}\right), & t_1 < t \leq t_2 \\ S_2^*(t). & t_2 < t \leq t_3 \end{cases}$$

The weight function is continuous with  $w(0) = 0$  and  $w(1) = 1$  to ensure that discontinuities are not introduced into  $S$ . We used  $w(x) = x$  as a simple and obvious choice.

More generally, suppose we want to reconcile signals  $S_1, \dots, S_n$  where  $S_j(t)$  is defined for  $t_{j-1} < t \leq$

$t_{j+1}$  and  $t_0 < t_1 < \dots < t_{n+1}$ . Then for  $j=1, \dots, n$  let  $l_j$  denote the mean of  $S_j$  over the interval  $(t_{j-1}, t_j]$  and let  $h_j$  denote the mean of  $S_j$  over the interval  $(t_j, t_{j+1}]$ .

$$S(t) = \begin{cases} S_1^*(t), & t_0 < t \leq t_1 \\ S_j^*(t) \left[ 1 - w \left( \frac{t - t_j}{t_{j+1} - t_j} \right) \right] + S_{j+1}^*(t) w \left( \frac{t - t_j}{t_{j+1} - t_j} \right), & t_j < t \leq t_{j+1}, j = 1, \dots, n-1 \\ S_n^*(t), & t_n < t \leq t_{n+1} \end{cases}$$

Define  $S_1^*(t) = S_1(t)$  and, for  $j=2, \dots, n$  define  $S_j^*(t) = S_j(t) - \sum_{i=2}^j (l_i - h_{i-1})$ . Finally, the resulting signal is given by

## References

- Bell, A., Sejnowski, T., 1995. An information-maximization approach to blind separation and blind deconvolution. *Neural Computation* 7, 1129–1159.
- Berg, P., Scherg, M., 1991a. Dipole models of eye movements and blinks. *Electroencephalography and Clinical Neurophysiology* 79, 36–44.
- Berg, P., Scherg, M., 1991b. Dipole modelling of eye activity and its application to the removal of eye artefacts from the EEG and MEG. *Clinical Physics and Physiological Measurement* 12 (Suppl. A), 49–54.
- Berg, P., Scherg, M., 1994. A multiple source approach to the correction of eye artifacts. *Electroencephalography and Clinical Neurophysiology* 90 (3), 229–241.
- Comon, P., 1994. Independent component analysis—a new concept? *Signal Processing* 36, 287–314.
- Croft, R.J., Barry, R.J., 2000. Removal of ocular artifact from the EEG: a review. *Neurophysiologie Clinique* 30, 5–19.
- deBoor, C., 1978. A practical guide to splines. *Applied Mathematical Sciences*, vol. 27. Springer-Verlag, New York, NY.
- DiMatteo, I., Genovese, C.R., Kass, R.E., 2001. Bayesian curve fitting with free-knot splines. *Biometrika* 88, 1055–1073.
- Elbert, T., Lutzenberger, W., Rockstroh, B., Birbaumer, N., 1985. Removal of ocular artifacts from the EEG—a biophysical approach to the EOG. *Electroencephalography and Clinical Neurophysiology* 60, 455–463.
- Fisch, B.J., 1991. Artifacts. In: Fisch, B.J. (Ed.), *Spehlmann's EEG Primer*, 2nd edition. Elsevier, Amsterdam, The Netherlands, pp. 108–124.
- Gratton, G., Coles, M.G.H., Donchin, E., 1983. A new method for the off-line removal of ocular artifact. *Electroencephalography and Clinical Neurophysiology* 55, 468–484.
- Hyvärinen, A., 1999. Fast and robust fixed-point algorithms for independent component analysis. *IEEE Transactions on Neural Networks* 10 (3), 626–634.
- Hyvärinen, A., Oja, E., 1997. A fast fixed-point algorithm for independent component analysis. *Neural Computation* 9 (7), 1483–1492.
- Jung, T.-P., Humphries, C., Lee, T.-W., Makeig, S., McKeown, M.J., Iragui, V., Sejnowski, T.J., 1998a. Extended ICA removes artifacts from electroencephalographic recordings. *Advances in Neural Information Processing Systems* 10, 894–900.
- Jung, T.-P., Humphries, C., Lee, T.-W., Makeig, S., McKeown, M.J., Iragui, V., Sejnowski, T.J., 1998b. Removing electroencephalographic artifacts: comparison between ICA and PCA. *Neural Networks for Signal Processing* 8, 63–72.
- Jung, T.-P., Makeig, S., Humphries, C., Lee, T.-W., McKeown, M.J., Iragui, V., Sejnowski, T.J., 2000. Removing electroencephalographic artifacts by blind source separation. *Psychophysiology* 37, 163–178.
- Jutten, C., Herault, J., 1991. Blind separation of sources: Part I. An adaptive algorithm based on neuromimetic architecture. *Signal Processing* 24, 1–10.
- Lagerlund, T.D., Sharbrough, F.W., Busacker, N.E., 1997. Spatial filtering of multichannel electroencephalographic recordings through principal component analysis by singular value decomposition. *Journal of Clinical Neurophysiology* 14 (1), 73–82.
- Lee, T.-W., Girolami, M., Sejnowski, T.J., 1999. Independent component analysis using an extended infomax algorithm for mixed sub-Gaussian and super-Gaussian sources. *Neural Computation* 11, 606–633.
- Lins, O.G., Picton, T.W., Berg, P., Scherg, M., 1993a. Ocular artifacts in EEG and event-related potentials: I. Scalp topography. *Brain Topography* 6 (1), 51–63.
- Lins, O.G., Picton, T.W., Berg, P., Scherg, M., 1993b. Ocular artifacts in recording EEGs and event-related potentials: II. Source dipoles and source components. *Brain Topography* 6 (1), 65–78.
- Makeig, S., Humphries, C., Jung, T.-P. et al., 1998. Ica toolbox for psychophysiological research. WWW Site, Computational Neurobiology Laboratory, The Salk Institute for Biological Studies, <http://www.cnl.salk.edu/scott/icadownload-form.html>.
- Marchini, J.L., Heaton, C., Ripley, B.D., 2002. The fastICA package. Software and documentation available at <http://www.stats.ox.ac.uk/marchini/software.html>.
- Miller, A., Fox, N.A., Cohn, J.F., Forbes, E.E., Sherrill, J.T., Kovacs, M., 2002. Regional patterns of brain activity in adults with a history of childhood-onset depression: Gender differences and clinical variability.
- Pivik, R.T., Broughton, R.J., Coppola, R., Davidson, R.J., Fox, N., Nuwer, M.R., 1993. Guidelines for the recording and quantitative analysis of electroencephalographic activity in research contexts. *Psychophysiology* 30, 547–558.
- Vigário, R.N., 1997. Extraction of ocular artefacts from EEG using independent component analysis. *Electroencephalography and Clinical Neurophysiology* 103, 394–404.
- Wallstrom, G., Kass, R., Miller, A., Cohn, J., Fox, N., 2002. Correction of ocular artifacts in the EEG using Bayesian adaptive regression splines. *Bayesian Statistics*, vol. 6. Springer-Verlag, New York, NY.